

Density Functional Study of Lithium–Aromatic Sandwich Compounds and Their Crystals

Hong Seok Kang*

College of Natural Science, Jeonju University, Hyoja-dong, Wansan-ku, Chonju, Chonbuk 560-759, Republic of Korea

Received: August 5, 2004; In Final Form: November 3, 2004

Using density functional theory, we have theoretically studied the formation of neutral lithium–aromatic complexes $R-n\text{Li}$ and $R-n\text{Li-R}$, where R is benzene, naphthalene, or pyrene. We first find that the maximum number of lithium atoms n in the complexes increases with the size of R. In addition, pyrene favors the sandwich compound $R-4\text{Li-R}$ over $R-4\text{Li}$ more than three times that of the corresponding tendency for benzene, strongly suggesting the possible existence of oligomer $(R-4\text{Li})_x$. We have also investigated energetics and band structures of infinite one-dimensional crystals of $R-n\text{Li}$, finding them metallic. Detailed analysis of the electronic structure shows that all these observations are related to the strong electrostatic interaction among the species, which is originated from the charge transfer from Li atoms to the aromatic rings. In addition, it is shown that the pyrene crystal is mechanically stable with respect to deformation. This also suggests the possibility of its existence, which, in turn, holds potential application in lithium storage in respect to its large Li/C ratio.

1. Introduction

For a long time, metal– π cation interaction has been known to be involved in various kinds of complexes. In relation to this, extensive investigations have been carried out for alkali metal cation– π complexes.^{1,2} Meanwhile, it was also found that not only the Li^+ ion but also the Li atom can make a sandwich complex of benzene with a large binding energy.³ More importantly, lithium is usually stored in the form of $R-n\text{Li}$ or $R-n\text{Li-R}$, not in the form of $R-n\text{Li}^+$ or $R-n\text{Li}^+-R$ in the lithium–ion battery, where R is graphite, disordered carbon, or potentially carbon nanotubes. This leads us to investigate physicochemical properties of neutral $R-n\text{Li}$ complexes and neutral $R-n\text{Li-R}$ sandwiches, where R is larger than benzene. In relation to this, we recall that the existence of naphthalene radical anion⁴ and naphthalene dianion⁵ have been known for a long time. In this work, we consider the case when R is either naphthalene or pyrene and estimate how its stability, the maximum number of Li atoms n , structure, and electronic properties depend on the size of the aromatic ring. To the best of our knowledge, there is only one theoretical work related to this problem, in which PM3 calculation was performed on the electron density distribution of HOMO for dianions R^{2-} in relation to the regioselectivity of alkylation of arenes.⁶ We have also studied the energetics as well as electronic properties of their one-dimensional (1D) crystals in which the sandwich structure is infinitely stacked along one direction. For this, we recall that some triple-decker sandwich compounds are known.^{7,8} Furthermore, we explore the mechanical stability of 1D crystal of pyrene with respect to sliding motion of a pyrene ring in order to evaluate the possibility of its real existence. All these calculations will give us a general idea on how extension of the π -system affects the binding of neutral alkali metals to the π -system.

2. Theoretical Methods

Our total energy calculations were performed using the Vienna ab initio simulation program (VASP)^{9,10} running on an

IBM-SP3 supercomputer. The electron–ion interaction is described by the projector augmented wave (PAW) method.¹¹ The exchange–correlation effect was treated within the generalized gradient approximation using the prescription proposed by Perdew, Burke, and Ernzerhof (PBE).¹² The solution of the KS equation was obtained using the Davison blocked iteration scheme followed by the residual vector minimization method.¹⁰ All the valence electrons of chemical elements were explicitly considered in the KS equation. For lithium, two 1s electrons were also included, although the 1s level lies far below the Fermi level of the system of concern. k -space sampling was done with Γ -point for molecular systems. Seven k -points were used for energetics of crystals along the crystal axis (= Z axis), while 15 points were employed for band structure calculations. The cutoff energy was set to 400 eV, and the conjugate gradient method was employed to optimize the geometry until force exerted on an atom was less than 0.04 eV/Å.

3. Results

We first consider $R\text{-Li-R}$ when R is a benzene molecule. Our calculation shows that all KS eigenstates are occupied up to $n = 32$, and the half-filled state at the Fermi level is derived from one of 2-fold degenerate LUMO levels of benzene molecules. (As in the case of B3LYP result, we do not observe Jahn–Teller distortion in our calculation.) This can be simply confirmed by noting that the total number of occupied states are originated from one 1s state of the Li atom, 12 C–C σ states, 12 C–H σ states, six π states of two benzene molecules, and one π^* state of a benzene molecule. Roughly speaking, there is only a shift of the Fermi level toward high energy compared to the case of an isolated benzene molecule. In fact, there still exists a large gap (= 4.27 eV) between HOMO-1 and HOMO, which can be reasonably compared with that (= 5.10 eV) between HOMO and LUMO of the benzene molecule. In fact, our analysis of electronic local density of states (LDOS) shows that the 2s state of the Li atom is found at +2.80 eV above the Fermi level, implying a complete charge transfer from 2s(Li)

TABLE 1: Binding Energies for the Reaction $R + n\text{Li} \rightarrow R-n\text{Li}$ (E_b^1) and $R + n\text{Li} \rightarrow R-n\text{Li-R}$ (E_b^2) Calculated from the Present Work and the Sum of the Two Energies Corresponding to the Overall Reaction $2R + n\text{Li} \rightarrow R-n\text{Li-R}$

R	n	E_b^1	E_b^2	$E_b^1 + E_b^2$
benzene	1	0.35	0.76	1.11
naphthalene	2	2.23	1.40	3.63
pyrene	4	3.93	2.72	6.65

to π_i^* (benzene). This is in excellent agreement with Vollmer et al.'s charge analysis, which showed that the natural bond order (NBO) charge of the Li atom [$= q(\text{Li})$] is $+0.917$.³ We have also calculated binding energies (E_b) of two reactions: $R(\text{singlet}) + \text{Li}(\text{doublet}) \rightarrow R\text{-Li}(\text{doublet})$ (reaction "B1") and $R\text{-Li}(\text{doublet}) + R(\text{singlet}) \rightarrow R\text{-Li-R}(\text{doublet})$ (reaction "B2"). Spin designation in parentheses indicates spin state which the corresponding species adopts in its ground state. For this, we have calculated the ground-state energy of each species from the spin-density calculation. Table 1 shows that the binding energies for the two reactions are 0.35 and 0.76 eV, in reasonable agreement with more sophisticated calculations. (Positive binding energy implies that a reaction is exothermic.) For this, we recall that the corresponding data are 0.25 and 0.72 eV from G3(MP2) calculations in ref 3. In all our data to be presented in this work, zero-point energy contributions are not included. A larger stabilization in the reaction B2 compared to that in B1 reflects strong electrostatic stabilization among $R^{-0.5}\text{-Li}^+\text{-R}^{-0.5}$. On the other hand, little charge transfer is expected from Li to R in the reaction B1, as evidenced by our separate analysis which shows that HOMO of R-Li mostly corresponds to the $2s(\text{Li})$ state. This is also consistent with Vollmer et al.'s NBO analysis which shows that the NBO charges of Li and R are practically zero in R-Li.³ Li–benzene distance ($= 1.898 \text{ \AA}$) and benzene–benzene distance ($= 3.796 \text{ \AA}$) are found to be almost the same as those from B3LYP/6-31G(d) calculations ($= 1.872$ and 3.744 \AA), also being in reasonable agreements with those ($= 1.769$ and 3.538 \AA) from MP2(FC)/6-31G(d) calculations.

We next consider the case when $R = \text{naphthalene}$. For this, we consider three reactions, i.e., $R(\text{singlet}) + \text{Li}(\text{doublet}) \rightarrow R\text{-Li}(\text{doublet})$ ($=$ reaction "N1"), $R\text{-Li}(\text{doublet}) + \text{Li}(\text{doublet}) \rightarrow R\text{-2Li}(\text{singlet})$ ($=$ reaction "N2"), and $R\text{-2Li}(\text{singlet}) + R(\text{singlet}) \rightarrow R\text{-2Li-R}(\text{singlet})$ ($=$ reaction "N3"). For R-2Li, we find that the anti conformation (singlet), in which two Li atoms are positioned on the opposite sides of different six-membered rings of the naphthalene ring, is more stable than the syn conformation (singlet) by 0.15 eV. Therefore, our energy calculations are based on the anti conformation of R-2Li. This implies that we assume that one of Li atoms rearranges itself so that it comes into the region between two R rings in the reaction N3. We find that R-2Li-R is in the singlet spin state. Our calculation shows that binding energies are 0.77, 1.46, and 1.40 eV for N1, N2, and N3, respectively. Table 1 summarizes this. We have already noted that both R-Li and R-2Li can be produced by exposing naphthalene to lithium metal. Although there has been no experimental report, our calculation shows that the naphthalene–Li system is more likely to exist in the form of the sandwich compound rather than existing as R-2Li, the tendency of which is stronger than the case of $R = \text{benzene}$. This observation gives us some preliminary information on similar compounds of large aromatic systems, the limiting case being the Li-intercalated graphite system. Figure 1 shows the optimized structure of R-2Li-R. We first find that two Li atoms do not lie on the top of the centers of hexagons. Each of them is displaced by 0.44 \AA toward C1 and C9 atoms, the reason for

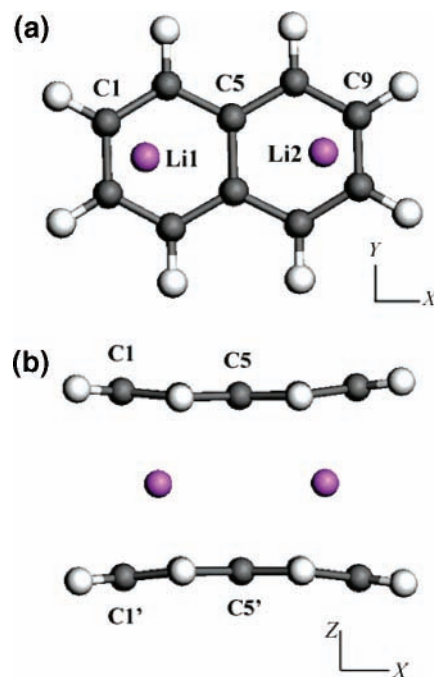


Figure 1. Views of R-2Li-R ($R = \text{naphthalene}$) projected onto XY and XZ planes.

which will be explained later in this paragraph. In addition, naphthalene rings are slightly bent. In fact, the interatomic distance between C5 and C5' is 3.698 \AA , while the corresponding distance between C1 and C1' is 4.019 \AA .¹³ This does not have anything to do with Jahn–Teller distortion, since molecular symmetry (D_{2h}) does not change upon deformation. We were able to confirm that Kohn–Sham HOMO of R-2Li-R has correct b_{3u} symmetry without degeneracy. We again note a gap ($= 2.29 \text{ eV}$) between HOMO-1 and HOMO originated from that [$= E_{\text{gap}}(\text{naphthalene}) = 3.41 \text{ eV}$] between HOMO and LUMO of the naphthalene molecule. However, the HOMO–LUMO gap ($= 0.81 \text{ eV}$) now becomes much smaller than $E_{\text{gap}}(\text{naphthalene})$. This is because it is originated from a weak $\pi^*-\pi^*$ interaction between two LUMOs of two naphthalene molecules. In other words, HOMO corresponds to their bonding interaction, while LUMO is characterized by the antibonding interaction. Weakness of the interaction can be understood, if we consider that the distance between two naphthalene rings does not allow large overlap between two π^* orbitals. Like the case of $R = \text{benzene}$, our analysis of l,m -projected LDOS shows that a state derived from $2s(\text{Li})$ is located about 2.80 eV above the Fermi level, clearly implying the charge transfer from the state to the lowest π^* state of naphthalene, converting it to HOMO upon complex formation. Therefore, large binding energy ($= 3.63 \text{ eV}$) of the overall process shown in Table 1 can be ascribed to the electrostatic interaction in $R^{-}\text{-2Li}^+\text{-R}^{-}$ as a result of charge transfer, which should be larger than that in $R^{-0.5}\text{-Li}^+\text{-R}^{-0.5}$ for $R = \text{benzene}$. In fact, our separate B3LYP/6-31G(d) calculation with GAUSSIAN program shows that $q(\text{Li}) = +0.904$, which is almost the same as the case of $R = \text{benzene}$ mentioned in the previous section. Interestingly, our analysis of LDOS also shows that the $2p_x(\text{Li})$ state interacts with HOMO, which should definitely contribute to the stabilization of HOMO with respect to LUMO. (See Figure 1 for definition of the coordinate system.) Now, we can explain the reason why two Li atoms do not sit on the top of hexagons. First, displacement would reduce the electrostatic repulsion between two positively charged Li ions. Second, Li ions would have a better electrostatic interaction with HOMO after charge transfer to it, which can be easily

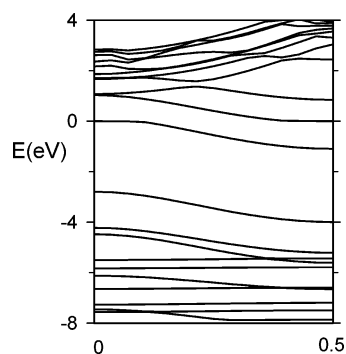


Figure 2. Band structure of the 1D crystal of R-2Li (R = naphthalene). Twenty-one bands around the Fermi level are shown. Note that the Fermi level is set to energy zero. The horizontal axis is in units of $2\pi/L_z$, where L_z is the lattice parameter along the periodic direction.

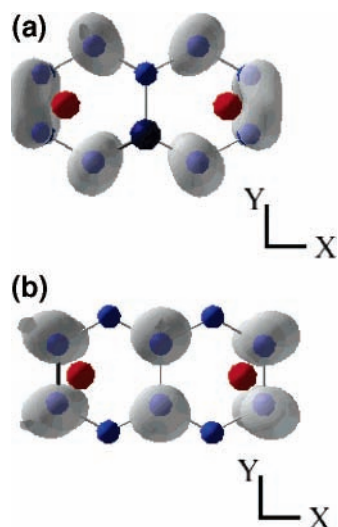


Figure 3. Electron density maps for HOMO(a) and LUMO(b) bands of the 1D crystal of R-2Li (R = naphthalene). For convenience, hydrogen atoms are not shown.

understood from the fact that HOMO has electron density more concentrated on C1 and C9, not on C5. This is also manifested in the NBO population analysis of this system, which shows that charges are -0.333 on C1 and C9, while it is -0.066 on C5. Third, a better interaction is expected between the π^* -(naphthalene) and $2p_x$ (Li) orbitals when a Li atom is displaced toward C1, contributing to an extra-stabilization. Note that we do not observe this kind of interaction in the case of R = benzene.

Next, we consider the one-dimensional (1D) crystal of $(R-2Li)_x$ (singlet), where R = naphthalene. The optimized lattice parameter along that axis was found to be 3.88 \AA , which lies between C1–C1' and C5–C5' distances in the sandwich R-2Li-R. At this time, we do not observe bending of naphthalene planes observed for R-2Li-R, i.e., they are planar in this 1D crystal. Thus, distortion of geometry in R-2Li-R merely reflects the surface effect. On one hand, Li atoms are displaced from the top of the centers of hexagons toward C1 and C9 by an amount ($= 0.44 \text{ \AA}$) which is the same as in R-2Li-R with R = naphthalene. The band structure in Figure 2 shows that this crystal is a zero-gap semiconductor. Figure 3 shows that HOMO and LUMO bands of this system are derived from LUMO and LUMO+1 of naphthalene. It is parallel to our finding that there is a complete charge transfer from a Li atom to the naphthalene ring for the sandwich R-2Li-R, since Figure 3 shows no appreciable charge density around Li atoms for HOMO of this crystal.

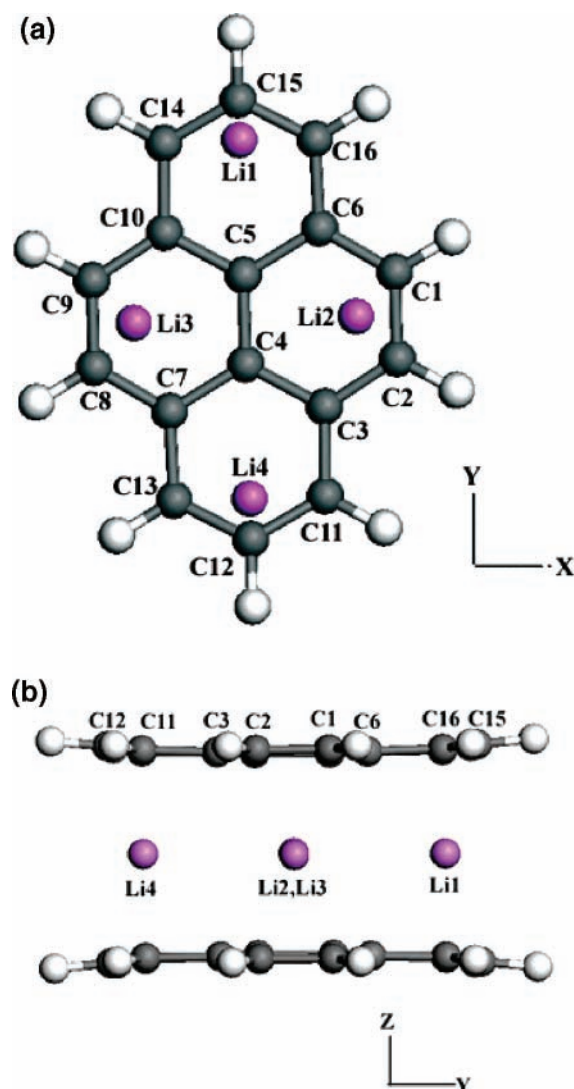
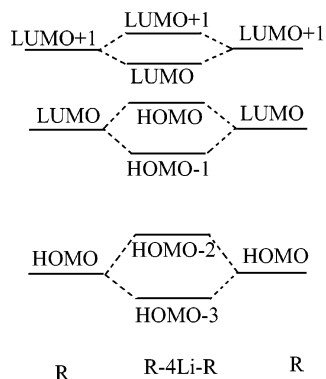


Figure 4. Views of R-4Li-R (R = pyrene) projected onto the XY and YZ planes.

Next, we consider the compound R-4Li-R where R = pyrene molecule. For this, we consider the reactions $R(\text{singlet}) + 4\text{Li}(\text{doublet}) \rightarrow R-4\text{Li}(\text{singlet})$ (reaction "P1") and $R-4\text{Li}(\text{singlet}) + R(\text{singlet}) \rightarrow R-4\text{Li-R}(\text{singlet})$ (reaction "P2"). In the complex R-4Li, it is assumed that two Li atoms, Li1 and Li4 in Figure 4a, are located on one side of the pyrene ring, and the other two, on the other side. Therefore, we are also assuming that two lithium atoms on the bottom rearrange themselves to move to the interior of the sandwich in the reaction P2. Table 1 shows that their binding energies are 3.93 and 2.72 eV , respectively. In fact, E_b for the reaction P1 is almost twice as large as that for the corresponding datum for naphthalene. In addition, the binding energy for the reaction P2 is more than three times of the corresponding datum [$= E_b(\text{B2})$] for benzene. Although our data may not be directly comparable to those from other kinds of calculation, such a comparison still gives us some idea on the binding strength of the sandwich formation, since our calculation on R-Li and R-Li-R (R = benzene) shows that our PBE calculation is nearly as reliable as more sophisticated calculations. For this, we note that $E_b = 1.18 \text{ eV}$ for the reaction $R-\text{Li}^+ + R \rightarrow R-\text{Li}^+-R$ (R = benzene) calculated from G3(MP2),³ implying that the reaction P2 is more favorable than this reaction. In other words, it is quite possible that R-4Li-R (R = pyrene) really exists and is stable at room temperature under the condition where the electron-transfer reaction is

SCHEME 1: Energy Level Diagram for HOMO-3–LUMO+1 of R-4Li-R in Relation to HOMO–LUMO+1 of R, Where R = Pyrene



quenched, considering that $R\text{-Li}^+\text{-R}$ ($R = \text{benzene}$) exists. In short, pyrene has the strongest tendency to form the sandwich compound in the presence of lithium atoms among all aromatic molecules studied. We also consider the reactions $2R(\text{singlet}) + 2\text{Li}(\text{doublet}) \rightarrow R\text{-}2\text{Li-R}(\text{singlet})$ (reaction “P’1”) and $R\text{-}2\text{Li-R}(\text{singlet}) + 2\text{Li}(\text{doublet}) \rightarrow R\text{-}4\text{Li-R}(\text{singlet})$ (reaction “P’2”), whose binding energies are found to be 3.41 and 3.24 eV, respectively. The reaction P’2 is energetically almost as much favorable as P’1, and the number of lithium atoms in the sandwich compound is expected to be at least 4. In relation to this, it was shown that arenes could also undergo dialkylation in the presence of lithium,⁶ which is expected to go through the formation of R-4Li.

Figure 4 shows the optimized structure of R-4Li-R. Lithium atoms are displaced from the centers of top of hexagons by an amount which is larger than those in $R = \text{naphthalene}$. Displacements are 0.68 Å for Li1 and Li4 and 0.64 Å for Li2 and Li3 along Y and X directions, respectively. Similar to the case of naphthalene analogue, these can be also expected from the electron density map of LUMO state of pyrene molecule, exhibiting electron density pronounced around peripheral atoms (C1, C2, C8, C9, C11, C13, C14, and C16). Here, we briefly describe the electronic structure of this system. Our careful analysis of l,m -projected LDOS of carbon atoms and electron density maps for the states HOMO-3–LUMO+1 of this system in comparison with HOMO–LUMO+1 of a pyrene molecule shows that a very simple model shown in Scheme 1 can be applied to this system around the Fermi level. Namely, interaction of two HOMOs of two pyrene molecules leads to HOMO-3 and HOMO-2 levels of the sandwich compound. Similarly, two LUMOs of pyrenes lead to HOMO-1 and HOMO and two LUMO+1 levels to LUMO and LUMO+1. This also signifies that the weak $\pi\text{-}\pi$ interaction does not introduce level crossing among these states upon dimer formation mediated by Li atoms. Levels HOMO-1 and HOMO are filled with electrons originated from $2s(\text{Li})$, again implying charge transfer of four electrons. Again, large overall binding energy ($= 6.65$ eV) of the overall process shown in Table 1 can be explained in terms of electrostatic interaction in $R^{-2}\text{-}4\text{Li}^+\text{-}R^{-2}$. The HOMO–LUMO gap ($= 0.23$ eV), which is originated from the LUMO–LUMO+1 gap of pyrene, is even smaller than that of its naphthalene analogue. We also note that HOMO-1 and HOMO have pronounced electron density on C11, C13, C14, and C16, while the density on C1, C2, C8, and C9 is lower than that in the LUMO of pyrene molecule. This is consistent with Herrera et al.’s PM3 calculation. In addition, our calculation also predicts that the regioselectivity of pyrene toward dialkylation would not be different from that toward monoalkylation.

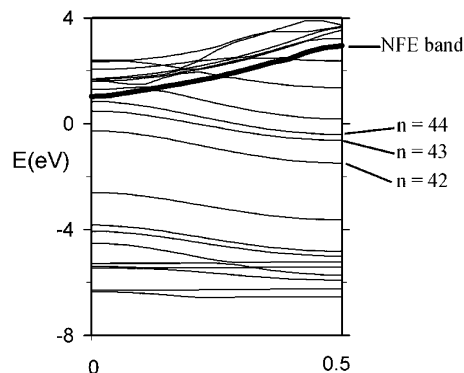


Figure 5. Band structure of the 1D crystal of R-4Li ($R = \text{pyrene}$). Twenty-one bands around the Fermi level are shown. Bands $n = 42\text{--}44$ are explicitly marked, and an NFE band is drawn with a thick line. Note that the Fermi level is set to energy zero. The horizontal axis is in units of $2\pi/L_z$, where L_z is the lattice parameter along the periodic direction.

Aromatic rings are also bent without breaking D_{2h} symmetry. Interatomic distances between equivalent atoms in two pyrene rings are 3.905 Å for C4–C4’, 3.946 Å for C3–C3’, 4.011 Å for C11–C11’, 4.201 Å for C12–C12’, and 4.206 Å for C1–C1’. Those in the center of the ring are closer to each other, while peripheral atoms are more separated from equivalent ones. In short, the pyrene rings are bowl-shaped with a larger inclination along X direction than along Y direction, and Li atoms sit on its convex sides.¹⁴ Since the LUMO level of the pyrene molecule is nondegenerate, this kind of deformation also does not have anything to do with Jahn–Teller effect.

Finally, we consider the 1D crystal of $(R\text{-}4\text{Li})_x$ (singlet) where $R = \text{pyrene}$. Optimal lattice constant along Z -axis ($= 3.88$ Å) is found to be the same as that for its naphthalene analogue, being slightly larger than the interlayer separation (~ 3.35 Å) in graphite. No deformation is observed in pyrene rings. The band structure in Figure 5 exhibits characteristics of a metallic system. It is similar to that for its naphthalene analogue in Figure 2 except that the pyrene crystal has one more state ($n = 44$) around the Fermi level. Analysis of the LDOS and the electron density map shows that bands $n = 42$ (filled), 43 (partially filled), and 44 (partially filled) are derived from LUMO (or HOMO-1 of R-4Li-R, equivalently), LUMO+1 (or LUMO of R-4Li-R, equivalently), and LUMO+2 of the pyrene molecule, also implying the charge transfer from four lithium atoms. We find a band with the character of nearly-free-electron (NFE) state crossing the band $n = 45$, which has electron density pronounced in the interstitial region along X and Y directions. For this, we recall that we have introduced large vacuum space along these directions in our supercell geometry. Considering that the NFE band lies at least 1.03 eV above the Fermi level with a large dispersion, we can expect that the electric conduction would mostly occur through the molecular framework along Z axis. In Figure 6, the electron distribution around Li2 and Li3 shows that $n = 43$ is a hybridization of LUMO+1(pyrene) and $p_x(\text{Li})$, again enhanced by displacements of the Li atoms toward C1, C2, C8, and C9. Partial filling of the bands $n = 43$ and 44 can be easily understood if we note that electron density is concentrated on carbon atoms C12 and C15 for $n = 43$, while it is concentrated on C1, C2, C8, and C9 for $n = 44$. In short, two of excess electrons from Li atoms cannot be solely accommodated by one of them, but should be distributed in the two bands. This also implies that it would not be possible to introduce more lithium atoms in the crystal, since it would result in large electrostatic repulsion between lithium ions in respect to the electron distributions in the two bands.

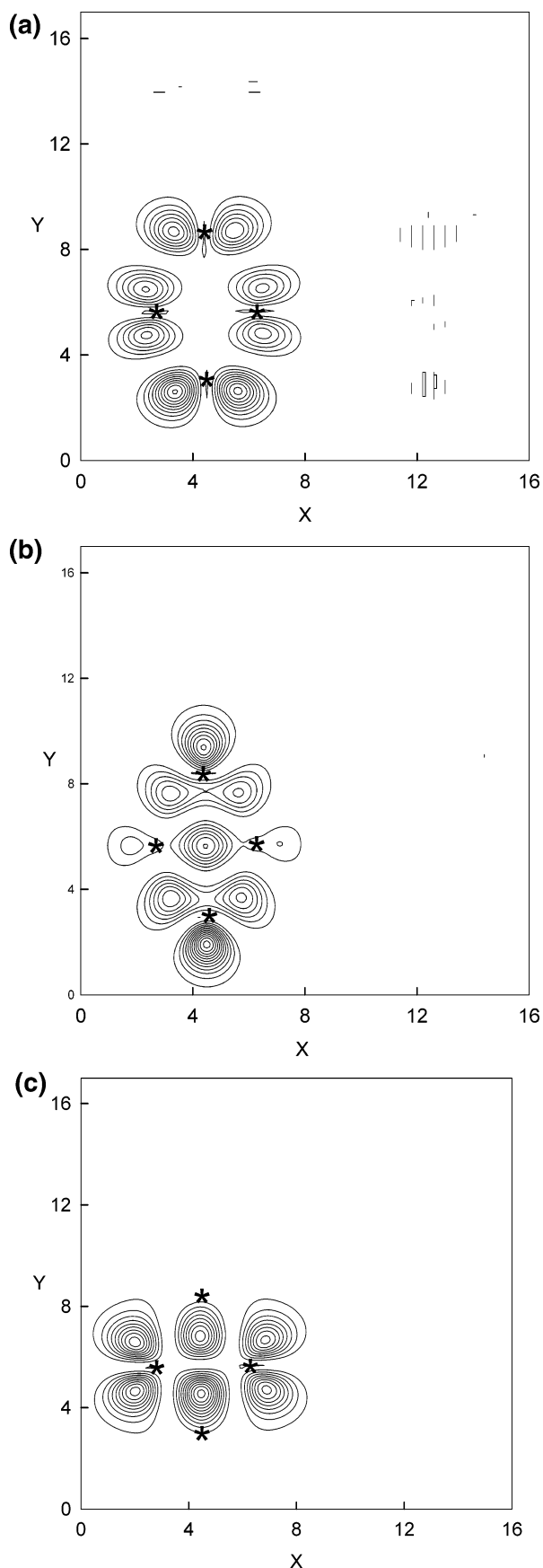


Figure 6. Electron density maps on the XY plane for the 1D crystal of $R-4Li$ ($R = \text{pyrene}$) at the value of Z corresponding to 0.3 \AA above the plane of pyrene ring. Three bands correspond to the band index $n = 42$ (a), 43 (b), and 44 (c). Positions of the lithium atoms are denoted by asterisk marks. Vertical bars around $X = 12$ are noises introduced by Fourier transformation.

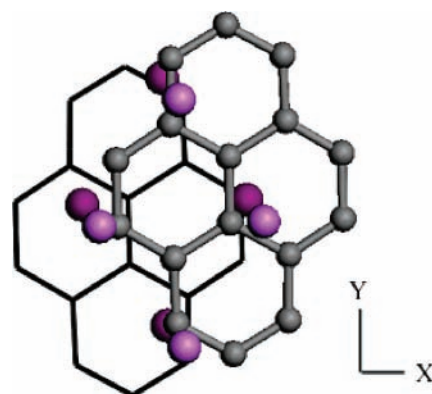


Figure 7. Initial structure of two units of $R-4Li$ ($R = \text{pyrene}$) in its 1D crystal where one of the pyrene rings (shown with ball-and-stick model) is displaced from its equilibrium position toward X and Y axis by 1.81 and 1.17 \AA , respectively. Eight lithium atoms are shown with large balls.

Here, we also study the mechanical stability of this system. For this, we have doubled the size of the supercell so that it includes two pyrene rings and eight lithium atoms. To examine the stability of the system with respect to the sliding motion of the crystal, one of the pyrene rings was artificially translated by a large amount, i.e., 1.81 \AA and 1.17 \AA toward X and Y directions from its equilibrium position. Lithium atoms were also assumed to be displaced from their equilibrium positions by $0.554\text{--}0.594 \text{ \AA}$ (see Figure 7). This configuration is far from equilibrium, since lithium atoms lie on the top of the boundary or the outside of one of two pyrene rings. Starting from this configuration, we were able to confirm that the time-consuming calculation for energy minimization indeed brings the system back to the structure of the perfect crystal. Total energy of the initial double-sized supercell was higher than the corresponding value at the equilibrium by 3.48 eV . This shows that the crystal is indeed elastic and stable with respect to the sliding motion. In fact, comparison of this value with $2E_{\text{lat}} (= 3.34 \text{ eV})$ to be discussed below shows that it is even more difficult to perform this kind of sliding deformation than to break the crystal into fragments of $R-4Li-R-4Li$. To estimate the stability of the 1D crystal with respect to the stretching motion along the periodic direction, we have calculated the lattice energy from a very stringent criteria, i.e., from the relation $E_{\text{lat}} = [E(R-4Li-R-4Li \text{ in crystal}) - E(\text{isolated } R-4Li-R-4Li)]/2$. This is because the process $R-4Li-R + 4Li \rightarrow R-4Li-R-4Li$ is quite exothermic with a large binding energy ($= 4.60 \text{ eV}$). We find that $E_{\text{lat}} = -1.17 \text{ eV}$, which gives a further stabilization so that it prefers the crystal in the form of $R-4Li-R-4Li$. It is also expected that the polymerization would greatly reduce the chemical reactivity of this system, since the inside of the crystal would be protected from the direct contact with other chemical reagents in view of the small lattice constant ($= 3.88 \text{ \AA}$).

4. Conclusions

Our calculation suggests that the tendency to form complexes of the form $R-nLi$ and $R-nLi-R$ increases with the size of the aromatic ring. Specifically, binding energy for the reaction $R+4Li \rightarrow R-4Li$ ($R = \text{pyrene}$) is six times as large as that for the corresponding process for benzene and twice as large as corresponding datum for naphthalene. In addition, binding energy for the reaction $R-4Li + R \rightarrow R-4Li-R$ ($R = \text{pyrene}$) is more than three times of that for the reaction $R-Li + R \rightarrow R-Li-R$ ($R = \text{benzene}$). Dimer $R-4Li-R-4Li$ and its 1D crystal are expected to be much more stable. For this, more careful

consideration might be necessary, since lithium–aromatic complexes may have several local minima with small energy difference between each conformer.

Band structure analysis shows that the crystal would exhibit metallic conduction. In addition, the crystal is found to be mechanically stable with respect to the sliding motion of pyrene ring, strongly suggesting the possibility of its existence. It would rather exist in the form of 3D crystal, and present analysis on 1D crystal will give us insight into the understanding of its physical properties. Without doubt, its benzene analogue, i.e., 1D crystal of benzene sandwich compound, would be unstable with respect to such a deformation, excluding the possibility of its existence. In fact, there is only one lithium atom bridging two benzene rings in the sandwich crystal, while there are four such atoms in its pyrene analogue. In short, we propose new organolithium complexes R-4Li, R-4Li-R, their oligomer (R-4Li)_x, and their crystal, where R = pyrene. Our calculation also suggests the possible existence of crystals of other aromatic compounds of even larger sizes. In addition, electronic properties of the complexes may be modulated by simply replacing lithium atoms by other kinds of metal atoms. For this, we note that transition metal–benzene complexes were prepared in gas phase using laser vaporization.¹⁵ Monomer or dimers of R-*n*Li for various kinds of R may find its applications in organic reactions, considering that naphthalene-2Li has been widely used for electron-transferring agent. We believe that the present work would stimulate experimental design and characterization of these complexes.

Meanwhile, this 1D crystal of pyrene is of special interest due to its large lithium-storage capacity. Considering its stoichiometry, C₁₆H₁₀Li₄, the capacity amounts to 25% of atomic percent with respect to the number of carbon atoms, which is larger than that for graphite (= 16%)¹⁶ and almost comparable to a recent report (= 33%) for single-wall carbon nanotubes (SWNT).¹⁷ Note that our calculation is focused on the R-*n*Li-R system and its 1D crystal, not on the R-*n*Li⁺-R system. It would not be easy for the latter system to form a 1D crystal similar to that discussed in this work, since it requires high density of negative ions around positive ions. For this, we note that the

lattice constant of 1D crystal is only 3.88 Å, and there should be four negative ions within a unit cell of this size in case of R-4Li⁺ crystal.

Acknowledgment. We thank Jeonju University for financial support.

References and Notes

- (1) (a) Larrivee, M. L.; Allison, J. *J. Am. Chem. Soc.* **1990**, *112*, 7134. (b) Wu, J.; Polce, M. J.; Wesdemiotis, C. *J. Am. Chem. Soc.* **2000**, *122*, 12786. (c) Nicholas, J. B.; Hay, B. J. *J. Phys. Chem. A* **1999**, *103*, 9815. (d) Amunugama, R.; Rodgers, M. T. *Int. J. Mass Spectrom.* **2003**, *222*, 431.
- (2) Gal, J.-F.; Maria, P.-C.; Decouzon, M.; Mo, O.; Yanez, M.; Abboud, J. L. M. *J. Am. Chem. Soc.* **2003**, *125*, 10394.
- (3) Vollmer, J. M.; Kandalam, A. K.; Curtiss, L. A. *J. Phys. Chem. A* **2002**, *106*, 9533.
- (4) Holy, N. L. *Chem. Rev.* **1974**, *74*, 243.
- (5) Smid, J. *J. Am. Chem. Soc.* **1965**, *87*, 656.
- (6) Herrera, R. P.; Guijarro, A.; Yus, M. *Tetrahedron Lett.* **2003**, *44*, 1313.
- (7) (a) Davis, J. H., Jr.; Sinn, E.; Grimes, R. N. *J. Am. Chem. Soc.* **1989**, *111*, 4776. (b) Duff, A. W.; Jonas, K.; Goddard, R.; Kraus, H. J.; Krueger, C. *J. Am. Chem. Soc.* **1983**, *105*, 5479.
- (8) (a) Wang, S.; Zhou, S.; Sheng, E.; Xie, M.; Zhang, K.; Cheng, L.; Feng, Y.; Mao, L.; Huang, Z. *Organometallics* **2003**, *22*, 3546. (b) von Hanisch, C.; Fesnske, D.; Weigend, F.; Alrichs, R. *Chem–Eur. J.* **1997**, *3*, 1494. (c) Benvenuto, M. A.; Sabat, M.; Grimes, R. N. *Inorg. Chem.* **1992**, *31*, 3904.
- (9) Kresse, G.; Hafner, J. *Phys. Rev. B* **1993**, *47*, RC558.
- (10) Kresse, G.; Furthmüller, J. *Phys. Rev. B* **1996**, *54*, 11169.
- (11) Kresse, G.; Joubert, D. *Phys. Rev. B* **1999**, *59*, 1758.
- (12) Perdew, J. P.; Burke, K.; Ernzerhof, M. *Phys. Rev. Lett.* **1996**, *77*, 3865.
- (13) Our PBE calculation shows that the corresponding distance in the benzene sandwich compound is 3.796 Å, still exhibiting *D*_{6h} symmetry overall.
- (14) It was shown that Li⁺ ion also prefers convex side when it binds to corannulene. See: Frash, M. V.; Hopkinson, A. C.; Bohme, D. K. *J. Am. Chem. Soc.* **2001**, *123*, 6687.
- (15) (a) Ma, J. C.; Dougherty, D. A. *Chem. Rev.* **1997**, *97*, 1303. (b) Dougherty, D. A. *Science* **1996**, *271*, 163. (c) Nakajima, A.; Kaya, K. *J. Phys. Chem. A* **2000**, *104*, 176.
- (16) Dresselhaus, M. S.; Dresselhaus, G. *Adv. Phys.* **1981**, *30*, 1399.
- (17) Shimoda, H.; Gao, B.; Tang, X. P.; Kleinhammes, A.; Fleming, L.; Wu, Y.; Zhou, O. *Phys. Rev. Lett.* **2002**, *88*, 015502.